Nominal PbSe nano-islands on PbTe: grown by MBE, analyzed by AFM and TEM

P. Moeck [1], M. Kapilashrami [1,2], A. Rao [1,2], J. Lee [3], J. Morris [3], N.D. Browning [4] and P. McCann [5]

[1] Department of Physics, Portland State University, Portland Oregon, [2] Department of Material Physics, Royal Institute of Technology, Stockholm, Sweden, [3] Department of Electrical and Computer Engineering, Portland State University, [4] Department of Chemical Engineering and Materials Science, University of California at Davis, [5] Department of Electrical and Computer Engineering, University of Oklahoma

Abstract

• Nominal PbSe nano-islands were grown in the Stranski-Krastanow mode on (111) oriented $PbTe/BaF_2$ pseudo-substrates by molecular beam epitaxy (MBE).

• The number density and height of these islands were assessed by means of atomic force microscopy (AFM). Transmission electron microscopy (TEM) was employed to determine the strain state and crystallographic structure of these islands.

• Transmission electron goniometry was employed to prove that the nano-island grew epitaxially in the halite structure.

• On the basis of both AFM and TEM we distinguish between different groups of islands. TEM indicated that there are also nm-sized entities that do not show strain fields, but superlattice reflection spots.

Introduction

Nano-islands general

• Currently most popular within the scientific community are nano-islands that are grown in the Stranski-Krastanow mode, where MBE and metal organic vapour phase epitaxy (MOVPE) are typically employed. Most nano-island work is on compressibly strained Ge island on Si, and various III-V and II-VI compound semiconductors with a focus on optoelectronics.

• The physics of nano-islands shows parallels to the behaviour of naturally occurring quantum systems such as atoms. The energy levels in a nano-island become quantized due to the confinement of electrons and holes.

• In this paper we present AFM and TEM results on tensibly strained PbSe nano-islands on $PbTe/BaF_2$.

PbSe nano-island growth

• The nominal PbSe islands on PbTe were grown by means of MBE at the University of Oklahoma using PbTe and PbSe sources. Freshly cleaved (111) oriented BaF_2 was used as substrate.

• After desorption of surface layers for 15 minutes at 500°C a 2.67 µm thick lattice matched $PbTe_{0.22}Se_{0.78}$ buffer layer was grown at 400°C with a growth rate of 0.278 nm/s.

• At 400 °C a 1.8 µm thick layer of Se doped PbTe was grown at a rate of 0.167 nm/s. Then the temperature was lowered to 380 °C and 2.6 monolayers (MLs) (i.e. approximately 0.8 nm) PbSe was deposited at a rate of 0.027 nm/s.

• The sample was finally cooled down to room temperature at a rate of 1K/s.

• [111] plane-view TEM specimens were prepared by standard mechanical grinding and ion-milling techniques. These specimens were analyzed in a JEOL JEM-3010 TEM at 300 kV at the Research Resources Center of the University of Illinois at Chicago.

AFM Analysis Results

Table 1 lists the mean heights, standard deviations, and relative spreads of three different groups of nano-islands as identified from height histograms (such as Fig. 1) of different areas. Small and large islands coexist in Figs. 2a and b and different areas have obviously different size distributions. A standard 10 nm radius of curvature scanning probe AFM tip was used for the acquisition of Figs. 2a,b. Significant convolution effects of the island topography and the shape of the AFM tip are present [1]. Consequently, the nano-islands appear shallower than they really are in Figs. 2a,b and their height to base widths (diameter) aspect ratio, Fig. 3, is smaller than that obtained by other authors [2-4] who used sharper scanning probe tips, Figs. 4a,b.

	Mean height h, (nm)	Standard deviation s, (nm)	Relative spread s/h, (%)	Density of islands, (mm^{-2})
All	18.704	9.804	52.42	158.3
small	8.154	1.619	19.85	14.6
medium	16.948	4.628	27.28	126.9
large	41.136	10.908	25.52	16.8

Table 1: *Investigated islands number: 1583 islands at 10 mm^2 selected area.*

The importance of a sharp tip when using AFM is clearly demonstrated in Figs. 2a,b, 4a,b, and 5. The true shape of PbSe nano-islands, Fig. 4a, is only revealed by scanning with (long and) ultrasharp tips (Pinczolits et al., Institute für Halbleiterphysik, Johannes Kepler Universität, Linz, Austria, see refs. [2,3] for details). If there were no islands-scanning tip convolutions in AFM images of PbSe nano-islands, a height to base widths (diameter) aspect ratio of $\sqrt{2}/3 \approx 0.471$ would be obtained, Fig. 3. For comparision, Fig. 5 was obtained at Portland State University with a so-called "sting tip" that is both longer and nominally sharper than the AFM tips used to record Figs. 2a,b.

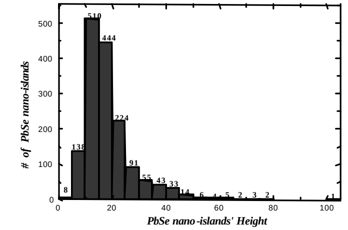

Fig 1. *Histogram of the PbSe nano-island.*

(a)

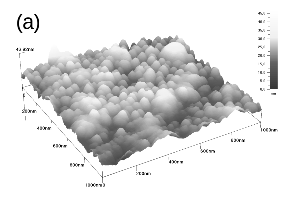

(b)

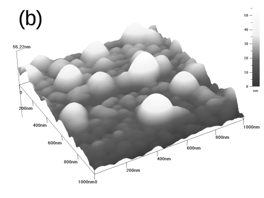

Fig. 2a,b *3D-AFM images of PbSe nano-islands; small and large islands coexist, different areas have different size distributions.*

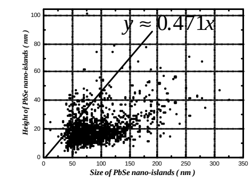

Fig. 3. *Measured PbSe nano-island height vs. diameter.*

(a)

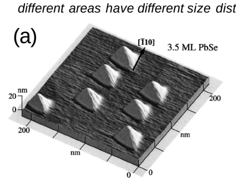

(b)

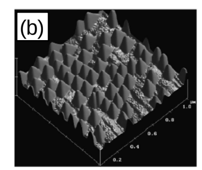

Fig. 4a: 3D-AFM image of PbSe nano-islands as obtained by the Linz group, ref. [2,3]; **4b:** *3D-AFM image of PbSe nano-islands as obtained by the Zurich group, ref. [4]. The mean nano-island height is 18.8 ± 0.6 nm in fig. 4b.*

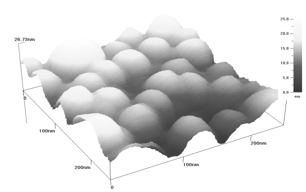

Fig. 5: 3D-AFM image of PbSe nano-islands taken with a so called "sting tip" (with aspect ratio of at least 4:1, > 600 nm extra tip height, and 5 to 10 nm typical radius of curvature.

TEM Analysis Results

• Fig. 6a shows larger (revealed by so-called "coffee-bean contrasts" and smaller (revealed by so-called "black-white" contrasts) PbSe nano-islands. According to the Ashby-Brown theory of strained precipitates, the difference in contrast are due to differences in size. The presence of strained nano-islands that can be classified into two different size groups is, thus, confirmed by TEM. As the contrast in these images shows, these two kinds of islands are obviously strained and we call them ordinarily strained nano-islands. They may be considered to constitute predecessors of ordinarily strained quantum dots.

• Fig. 6b shows a small region of the wetting layer between islands in high-resolution in the [111] zone axis orientation. Three approximately 0.22 nm wide ± {-220} lattice spacings reveal the [111] zone-axis pattern of a crystal with halite structure. This is clearly resolved in both the image and the its insert Fourier transform power spectrum. Tilting the crystal anticlockwise around the (-220) net-plane normal by an amount of approximately $\arccos(4/\sqrt{6}\cdot\sqrt{3}) \approx 19.47°$ from the goniometer setting a = -2.8°, ß = 6.1° of the double-tilt holder (as indicated in fig. 6b) to the goniometer setting a = 16.5°, ß = 4.7° resulted in a <112> zone axis being visible, fig. 6c. ***This is an example of transmission electron goniometry [5].*** The [-110] direction was fortunately close to the eucentric axis of the double-tilt holder, aiding the experimental tilting procedure greatly.

Fig. 6c shows both lattice fringes and "pseudo black-white" contrast as this high-resolution phase contrast image was taken from an area that showed "black-white" contrast in the diffraction contrast mode, indicating the presence of a small strained PbSe island. The approximate lattice spacings in this image are 0.22 nm for ± (-220) and 0.36 nm for ± (11-1). The [112] zone axis pattern of a crystal with halite structure has, thus, been adjusted by the transmission electron goniometry procedure. All of the crystallographic observations are consistent with the fact that both the Pb(Se,Te) wetting and buffer layers and the PbSe nano-islands possess the halite (rock salt) structure, as one would expect it to be for epitaxial growth.

• Adjacent to the areas with ordinarily strained nano-islands, there were specimen regions that showed under the same imaging condition contrasts that are probably mainly due to absorption differences, Fig. 7a. We suggest that these entities possess significantly higher Te contents than the surrounding matrix and are atomically ordered.

• Consistent with our hypothesis on atomic ordering, the selected areas electron diffraction pattern of the same area showed a variety of super-lattice reflections, Fig. 7b, that cannot arise from a crystal with the halite structure. Corresponding super-lattice reflections were also observed in Fourier transform power spectra of [111] and [112] zone-axis high-resolution phase-contrast images from the same specimen region.

(a)

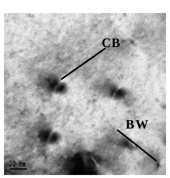

Fig. 6(a) *Near <111>, {220} dark field diffraction contrast image of smaller and larger ordinarily strained PbSe quantum dot predecessor islands.*

(b)

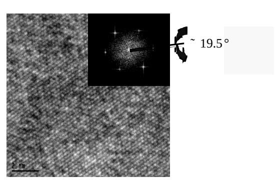

Fig. 6(b) *[111] zone axis, high-resolution phase-contrast image with insert Fourier transform power spectrum. Goniometer setting:* a = -2.8°, ß = 6.1°.

(c)

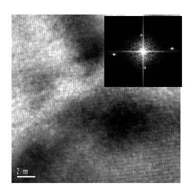

Fig. 6(c) *[112] zone axis, high-resolution phase-contrast image with insert Fourier transform power spectrum. Goniometer setting:* a = 16.5°, ß = 4.7°.

(a)

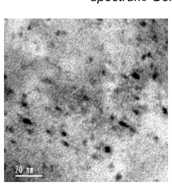

Fig. 7(a) *Near <111> {220} bright field diffraction contrast image of PbSe. There are no "black-white" and "coffee-bean" contrasts which would identify strain fields.*

(b)

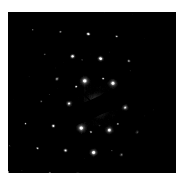

Fig. 7(b) *<111> zone-axis selected area electron diffraction pattern showing a variety of superlattice reflections (some marked by arrows) that we assume to be due to Pb-Se-Te compounds.*

Summary

• The coexistence of smaller and larger ordinarily strained PbSe nano-islands, i.e. ordinarily strained QD predecessor structures, was observed by both AFM and TEM.

• The dominant variety of nano-islands possesses an average height of approximately 16.9 nm with a standard deviation of 4.6 nm and a relative spread of 27.3 %. Regions with small atomically ordered entities that consist probably of atomically ordered Pb-Se-Te compounds were also identified in the same specimen. These islands may be considered as constituting predecessors of atomically ordered quantum dots.

References

[1] J.G. Griffith and D.A. Grigg, Dimensional metrology with scanning probe microscopes, J. Appl. Phys. **74**, R83 (1993).
[2] M. Pinczolits, G. Springholz, and G. Bauer, Direct formation of self-assembled quantum dots under tensile strain by heteroepitaxy of PbSe on PbTe (111), Appl. Phys. Lett. **73**, 250 (1998).
[3] M. Pinczolits, G. Springholz, and G. Bauer, Molecular beam epitaxy of highly faceted self-assembled IV–VI quantum dots with bimodal size distribution, J. Cryst. Growth **201-202**, 1126 (1999).
[4] K. Alchalabi, D. Zimin, G. Kostorz, and H. Zogg, Self-assembled semiconductor quantum dots with nearly uniform sizes, Phys. Rev. Lett. **90**, 26104 (2003).
[5] P. Moeck, W. Qin, and P. Fraundorf, Image-based Nanocrystallography by means of Transmission Electron Goniometry, Proc. 4th World Congress of Nonlinear Analysts, Symposium on Nanoscience and Nanotechnologies in Engineering Problems & Systems, June 30 - July 7, 2004, Orlando, Florida,
and http://www.physics.pdx.edu/~pmoeck/goniometry.htm